immunohistochemically confirmed using anti-α-synuclein antibodies. Sections were then stained for phosphorylated α-synuclein with psyn#64, and based on this staining, a new LB score was calculated using the same criteria referenced above. Selected sections were also stained with polyclonal anti-psyn antibody (13) to confirm the results obtained with monoclonal psyn#64. Small pieces of brain with abundant LB-related pathology were directly fixed in 2.5% glutaraldehyde, postfixed in 1% osmium tetroxide, embedded in epon, and examined in an electron microscope (Hitachi 7500, Hitachi, Japan).

RESULTS

Neuropathology

The 157 serial autopsy brains examined here included 47 cases of neurodegenerative disorders: 15 cases of AD, 13 cases of dementia with grains (DG), 4 cases of DLB neocortical form, 5 cases of DLB transitional form, 2 cases of Parkinson disease, 3 cases of progressive supranuclear palsy (PSP), 1 case of corticobasal degeneration, 1 case of neurofibrillary tangle-predominant form of dementia (NFTD), 1 case of PSP plus DG, 1 case of NFTD plus DG, and 1 case of AD plus DG. All 5 cases with DLB transitional form were categorized as Parkinson disease with dementia, according to McKeith et al (i.e. the onset of dementia was more than 1 year later than the development of parkinsonism) (6, 15). In 3 of the 15 AD cases, LBs were preferentially present in the amygdala; they were abundant in 2 cases and scattered in the third. One case was consistent with LB-related dysphagia (5), with LBs and gliosis preferentially involving the dorsal motor nucleus of the vagus.

Based on examination with H&E staining and immunohistochemistry with anti-ubiquitin antibody, the 157 brains were classified into the following 5 categories: Stage 0: no LBs (128 cases); Stage I: scattered LBs without cell loss (9 cases); Stage II: abundant LBs with macroscopic loss of pigmentation in substantia nigra and locus ceruleus and/or gliosis demonstrated by GFAP immunohistochemistry in the areas containing LBs but without attributable parkinsonism or dementia (9 cases); Stage III: Parkinson disease (2 cases); Stage IV: DLB, transitional form (5 cases); and Stage V: DLB, neocortical form (4 cases).

Characterization of Anti-Phospho-α-Synuclein (psyn) Antibody

Western blotting of the differential extracts from DLB and control brains revealed a ~15 kDa polypeptide that was labeled by a human-specific anti α-synuclein antibody (LB509) (3). The polypeptide was detected in TX-soluble fractions from DLB and normal control brains and represents normal α-synuclein, as previously reported (13) (Fig. 1). A major ~15 kDa polypeptide and a minor additional higher molecular weight polypeptide, which may correspond to ubiquitinated α-synuclein species (16), were detected by LB509 in Sarkosyl-insoluble, urea-soluble fractions from DLB cortices. Monoclonal antibody (mAb) psyn#64 did not label TX-soluble α-synuclein, but strongly reacted with the urea-soluble α-synuclein in DLB brains in an identical pattern to that observed using a phosphorylated Ser129-specific polyclonal antibody, (anti-PSer129) (3). Given that urea-soluble α-synuclein in DLB brains is highly phosphorylated at Ser129 and Tris/TX-soluble normal α-synuclein is not (3), the data are consistent with mAb psyn#64 reacting similarly to anti-PSer129, with the phosphorylation-dependent epitope around PSer129 of α-synuclein. On Western blotting of recombinant human α-synuclein, mAb psyn#64 recognized α-synuclein phosphorylated at Ser129 by casein kinase 2 (data not shown) but did not recognize nonphosphorylated α-synuclein.

Anti-Phospho-α-Synuclein (psyn) Immunopathology

Immunohistochemical staining with anti-α-synuclein (LB509 and S1) antibodies improved both the specificity and the sensitivity for LB-related pathology, as compared to anti-ubiquitin immunohistochemistry, but was seriously complicated by diffuse staining of the background with a synaptic, cytoplasmic, or axonal pattern. The background staining was especially pronounced in paraformaldehyde-fixed sections. Occasional spheroids in the amygdala and zona reticulata of the substantia nigra were also moderately immunoreactive with LB509 and S1.

In contrast, immunostaining with mAb psyn#64 did not produce background staining or anti-α-synuclein-immunoreactive spheroids. The mAb did reveal, however, positively staining Lewy dots (Fig. 2A, E, F) and Lewy threads (Fig. 2A, F) in association with LBs (Fig. 2E, F). These immunopositive dots and threads were best visualized in paraformaldehyde-fixed tissues but could also be detected in buffered-formalin-fixed tissues. Focal enlargement along the course of threads, which corresponded to Lewy neurites in adjacent anti-nonphosphorylated α-synuclein-stained sections, was frequently seen (Fig. 3D). The process of LB formation in pigmented neurons of the substantia nigra appeared to progress from faint (Fig. 2B) or intense (Fig. 2C) diffuse cytoplasmic staining (pre-LB) to single or multiple (Fig. 2D) focal cytoplasmic aggregates (corresponding to pale bodies) to typical positive rings with negative cores (corresponding to brainstem-type LBs) (Fig. 2E). Cortical LBs showed a similar process of progression from focal cytoplasmic accumulations of the epitope to round inclusions (Fig. 2F) with or without central pallor. Immunoreactive glial inclusions were occasionally observed among these neuronal lesions (Fig. 2E, G).

Anti-psyn immunohistochemistry also revealed intense immunoreactivity in the alveus in the subcortical area of the anterior subiculum (Fig. 3A, C), where abundant cortical LBs were present. Additionally, there was staining

in the white matter around the amygdala (Fig. 2G) and in the subcortical white matter of the anterior cingulate gyrus.

With confocal microscopy, anti-psyn immunoreactivity in the white matter was almost exclusively colocalized with the epitope of SMI 31 (Fig. 4A–C). In contrast, Lewy dots and threads in the gray matter were partially colocalized with the epitope of anti-MAP2 (Fig. 4D–F) or SMI 31 (data not shown).

Anti-psyn-immunoreactive structures were observed in 11 of the original Stage 0 cases, preferentially in the dorsal motor nucleus of the vagus and medullary reticular formation in 9 cases and in the amygdala in 2 cases (1 AD case and 1 cognitively normal case with grains (CNG) (14). Five of these 11 cases contained only Lewy dots and threads, but no perikaryal immunoreactivity (4 cases with immunoreactivity in the dorsal motor nucleus of vagus or medullary reticular formation and 1 case of AD with immunoreactivity in the amygdala). We included the 6 cases with perikaryal pre-LBs in a new Stage 1 and categorized the 5 cases with only threads and dots into a new Stage 0.5 (Table 1).

Thirteen of the 15 cases that were newly classified as Stage I with anti-psyn immunohistochemistry had positive staining most prominent in the medulla oblongata. The immunoreactivity was exclusively there in 2 cases, extended to the substantia nigra in 4 cases, and extended to the limbic structure in 7 cases. The remaining 2 cases had AD and showed neuronal intracytoplasmic staining exclusively in the amygdala. Some cases also showed focal aggregates of anti-psyn epitope in the inferior olivary nucleus (Fig. 3F), along with positive dots and threads in the dentate nucleus.

The original Stage II cases were newly subclassified into 2 groups: limbic (IIL, 4 cases), and neocortical variant (IIN, 5 cases), based on the new LB scores calculated with anti-psyn immunohistochemistry. Tables 2A and 2B summarize the cases in the original categories II-V based on examination with H&E and anti-ubiquitin antibody. Two AD cases (Cases 14 and 17 that had preferential involvement of the amygdala were classified into IIL (Case 17) and IIN (Case 14) and showed minor but not negligible positive immunoreactivity in the substantia nigra and dorsal motor nucleus of the vagus. These 2 AD cases contained anti-psyn-immunoreactive neuritic plaques and tangles in the amygdala, entorhinal cortex, and prosubiculum. The colocalization of the epitope of phosphorylated tau and psyn was frequent in the sections immunostained for both psyn#64 and AT8 (data not shown). One case of PSP also had preferential involvement of the amygdala, although anti-psyn-immunoreactivity was detected in all areas showing tauopathy, including the posterior horn of the spinal cord (17). In the amygdala, AT8-immunoreactive threads outnumbered psyn#64-immunoreactive threads and were rarely colocalized together in double-immunostained sections (data not shown). All cases of Stages IIL and IIN showed many LBs and Lewy neurites associated with dots in the transentorhinal area, as well as many Lewy neurites and pre-LBs in CA2 and CA3. Thick neurites, which were strongly immunoreactive with anti-psyn, clustered in the molecular layer of the anterior subiculum,. These thick neurites were most prominent in Stage V cases (Fig. 3B), but they were also seen in 1 of 4 cases of Stage IIL and all cases of Stage IIN. Some of these neurites were identified as intraneuritic LBs in the adjacent H&E-stained sections.

Stage III cases presented with definite limbic pathology involving the transentorhinal area, CA2, CA3, and amygdala. The clustered thick Lewy neurites in the molecular layer of the anterior subiculum were seen in all Stage III cases and were more conspicuous than in the Stage II cases. The involved temporal neocortex had numerous cortical LBs and neurites surrounded by dots and threads. Lesions involving hippocampal CA2 and CA3 were observed in all Stage III cases. The lesions gradually decreased in severity from frontal to parietal cortex, although number of anti-psyn-immunoreactive LBs or intraneuronal aggregates of psyn-immunoreactivity in parietal cortex were still sufficiently numerous for a score of 2, based on the published consensus guidelines (6).

Stage IV cases showed considerable anti-psyn immunoreactive structures in frontal neocortex, including the molecular layer, and in temporal neocortex. There was moderate immunoreactivity in the parietal cortex and mild immunoreactivity in the occipital cortex and striatum. The entorhinal and transentorhinal cortex showed spongiosis associated with numerous Lewy dots and accompanied by psyn-immunoreactive tangles. Approximately 10% of these tangles were also AT8-immunoreactive in double-immunostained sections (data not shown). The lesions in hippocampal CA2 and CA3 were more severe than those in Stage III cases.

Stage V cases showed more widespread neocortical involvement by anti-psyn immunoreactive structures and by degeneration in the limbic system. The lesions in CA2 and CA3 (Fig. 3D) and the spongiosis with numerous Lewy dots in the entorhinal and transentorhinal areas were more conspicuous in Stage V than Stage IV. Psyn-immunoreactive tangles were also more frequent in Stage IV. Scattered neuropil threads, which were immunoreactive for both AT8 and psyn#64, were present in double-immunostained sections (data not shown). The lesions were also more prominent in Stage V than in Stage IV in the cingulate gyrus, insular cortex and entire medial temporal lobe, and frontal and parietal cortex. Numerous Lewy dots were seen in the putamen, with a ventrolateral to dorsomedial gradient (Fig. 3E). Abundant Lewy dots and threads were also detected in the molecular layer of the affected cortical structures,

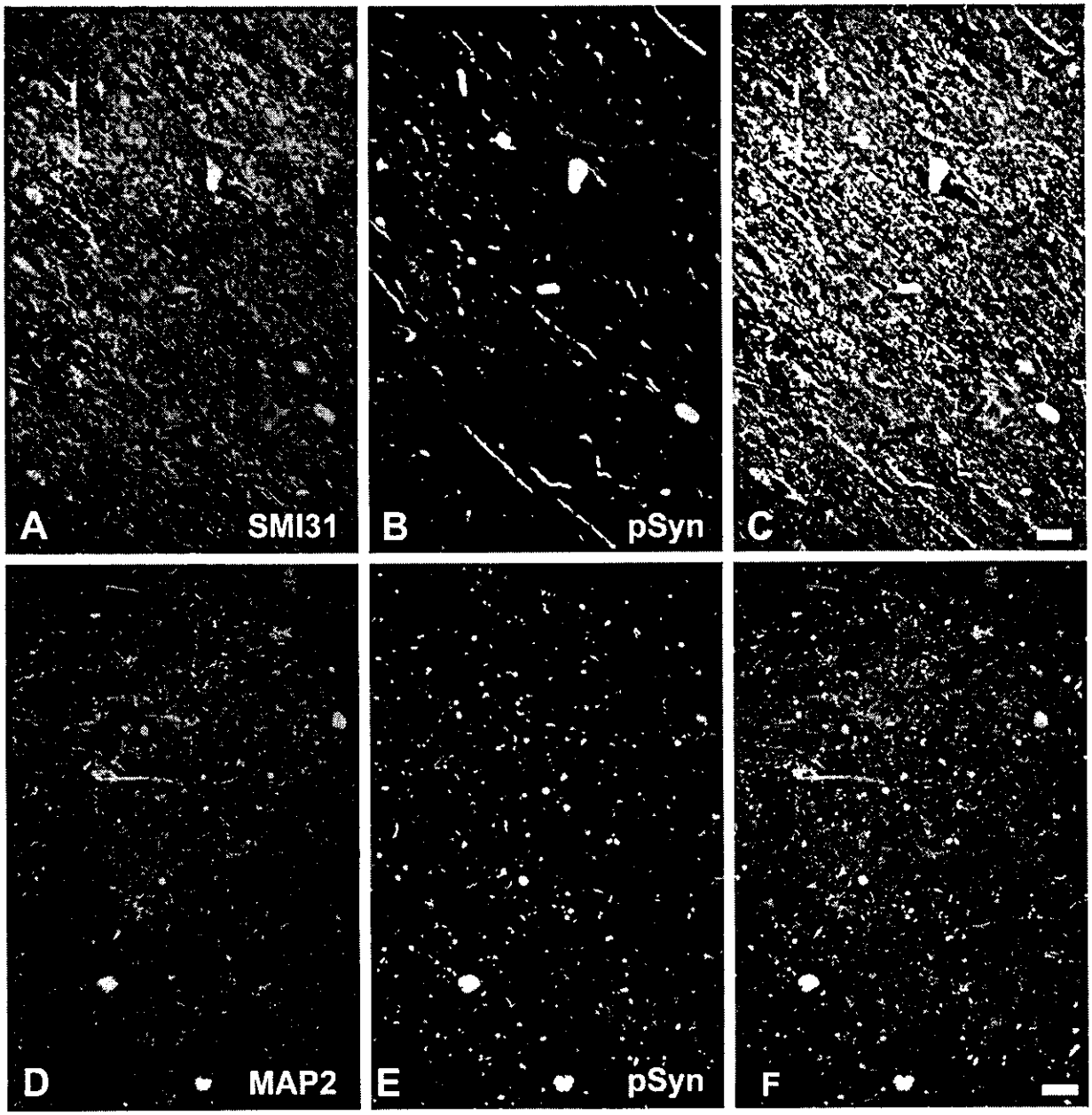

Fig. 4. Axonal and somatodendritic localization of phosphorylated α-synuclein. Sections of amygdala were double immunostained with polyclonal anti-phosphorylated -synuclein antibody (anti-PSer129) and with anti-phosphorylated neurofilament (SMI 31) (**A–C**) or anti-MAP2 (HM-2) (**D–F**). The primary antibodies were visualized with anti-rabbit Alexa 568 Fluor™ (red) and anti-mouse IgG Alexa 488™ (green) (Case 2). **A–C:** Confocal image of the white matter of the amygdala (the same area as Fig. 2F). The epitope of anti-Pser129 (red) is almost exclusively colocalized with that of SMI 31 (green). Anti-Pser129-immunoreactive axonal swellings are scattered. **D–F:** In the amygdala proper, some anti-Pser129-immunoreactive dots and threads (red) are colocalized with the epitope of anti-MAP2 antibody (green). **A, D:** Alexa 488 (green) for phosphorylated neurofilament (**A**) or MAP2 (**D**). **B, E:** Alexa 568 (red) for polyclonal phosphorylated α-syncuclein, anti-Pser129. **C, F:** Merged views for (**A/B**) and (**D/E**). Scale bar = 20 μm.

including the occipital cortex (Fig. 3G). In the sections double-immunostained for both psyn#64 and anti-Aβ 11–28, almost all senile plaques contained anti-psyn-immunoreactive dystrophic neurites in the areas where the immunoreactivity with anti-psyn was abundant. Although very small in number, some amyloid cores appeared to contained the epitope of psyn.

Electron microscopic observation of the molecular layer of the anterior subiculum confirmed the presence of intraneuritic Lewy bodies. Ultrastructurally, the Lewy

TABLE 1
Early Lewy Body-Related Pathology Detected with Anti-Phosphorylated α-Synuclein Immunohistochemistry

Age (yr)	Sex	Neurological diagnosis	Pathological diagnosis	Distribution and extent					Original staging of Lewy body
				DMNX	RF	LC	SN	Amy	
Stage 0.5									
93	F	Dementia	DG	+−	−	+−	−	−	0
69	M	Unremarkable	Unremarkable	−	+−	−	+−	−	0
98	F	Dementia	DG	+−	+−	−	+−	+−	0
76	M	Unremarkable	Unremarkable	+−	+−	+−	+−	+−	0
86	M	AD	AD	−	−	−	−	+−	0
Stage I									
73	F	CVD	CVD	+	−	−	−	−	0
86	M	Unremarkable	Unremarkable	+	+	+−	−	+−	0
88	F	Hepatic coma	Unremarkable	+	+	−	+	+−	0
78	F	Dementia	DG/ NFTD	+	+	−	+−	+−	0
94	F	CVD s/o	CVD	+−	+	++	−	++	0
72	M	Unremarkable	CNG	−	+−	−	−	+	0
70	M	Unremarkable	Unremarkable	+−	+	++	+	+−	I
69	M	CVD, dementia	VD	++	+	++	+	+−	I
84	F	Unremarkable	Unremarkable	++	++	++	++	++	I
82	M	Unremarkable	CVD	++	++	++	++	+	I
78	M	Unremarkable	Unremarkable	+	+	++	+	+	I
80	M	Unremarkable	Unremarkable	++	+	+	+	++	I
78	M	Dementia	DG/ CVD	+	++	−	+	++	I
98	M	AD	AD	+−	−	−	+−	+	I
78	M	AD	AD	+−	+−	−	−	+	I

Abbreviations: DMNX, dorsal motor nucleus of vagus nerve; RF, reticular formation in the medulla oblongata; LC, locus ceruleus; SN, substantia nigra; Amy, amygdala; DG, dementia with grains; AD, Alzheimer disease; CVD, cerebrovascular disease; NFTD, neurofibrillary tangle-predominant form of dementia; CNG: cognitively normal case with grains (14); and VD, vascular dementia. Extent of antiphosphorylated α-synuclein immunoreactive structures are as follows: −, none; +−, dots and threads only; +, intraneuronal (perikaryal) presence of the epitope; ++, dense aggregates of the epitope in the neuronal cytoplasm.

bodies presented as large spherical amorphous cores of high electron density surrounded by meshworks of granulofilamentous profiles (not illustrated).

DISCUSSION

The present study revealed 4 new findings: 1) phosphorylation of α-synuclein (psyn) occurred in about one fourth of the aged population; 2) anti-psyn immunocytochemistry allowed novel visualization of pre-LBs as well as Lewy threads, dots, and axons; 3) α-synucleinopathy begins in the medulla oblongata if it is an independent disease process, or in the amygdala if associated with AD; and 4) severe neocortical involvement by psyn is present in the medial temporal lobe in Parkinson disease, extends to the frontal lobe in DLB transitional form, and additionally involves the parietal and occipital lobes in DLB neocortical form.

We believe that our autopsy series is reasonably representative of the general older population in Japan. The 157 brains we examined are from a serial autopsy series at TMGH. This is one of the oldest and largest public geriatric hospitals in Japan, with 900 outpatients daily and a 700-bed ward. Every effort is made to secure postmortem neuropathological examinations on all patients dying at TMGH, whether or not a neurological disease was diagnosed antemortem. The autopsy rate was 32% during the period of this study.

Anti-psyn immunohistochemistry resulted in better visualization of previously reported LB-related pathology, except in a few anatomical loci such as the inferior olivary nucleus and occipital cortex. Using this more specific and sensitive marker, we found that 25 percent of the cases in our serial autopsy series had LB-related pathology. The limbic pathology specifically linked to DLB was detected in apparently presymptomatic cases, suggesting that phosphorylation of α-synuclein at Ser129 represents a pathological change that precedes LB-related neuronal degeneration. The pre-LBs, Lewy threads, and Lewy dots detected with anti-psyn immunohistochemistry are morphologically analogous to the pretangles, neuropil threads, and argyrophilic grains (18) detected with anti-phosphorylated tau immunohistochemistry. The Lewy threads were thinner and shorter than the Lewy neurites detected with anti-ubiquitin or anti-α-synuclein

TABLE 2A
Clinical Profiles of the Cases Showing Lewy Body-Related Neuronal Degeneration

Case	Age (yr)	Sex	Neurological diagnosis	CDR	PA	Dementia	Pathological diagnosis
1	85	M	PD+AD	3	10 yr	2 yr	DLBN
2	83	F	DLB	1	(–)	>2 yr	DLBN
3	92	F	Senile dementia	3	(–)	>2 yr	DLBN
4	77	M	DLB	3	2 yr	6 yr	DLBN
5	88	M	PD+dementia	1	11 yr	4 yr	DLBT
6	85	F	PD+dementia	1	19 yr	5 yr	DLBT
7	85	M	Drug-induced PA	1	>1 yr	n.d.	DLBT
8	86	F	PD+dementia	2	20 yr	1.75 yr	DLBT
9	79	F	PD+dementia	2	8 yr	>1 yr	DLBT/Fahr
10	79	M	PD	0	>20 yr	(–)	PD
11	77	M	PD	0	>1 yr	(–)	PD
12	84	M	MCI	0.5	(–)	2 yr	Early DLBT?
13	80	F	Unremarkable	0	(–)	(–)	CVD
14	90	F	Senile dementia	1	(–)	0.5 yr	AD/ CS
15	86	F	Unremarkable	0	(–)	(–)	Unremarkable
16	90	F	Senile dementia	1	(–)	>2 yr	DG
17	79	F	FTD	2	(–)	14 yr	AD
18	80	F	Dysphagia	0	(–)	(–)	Lewy body dysphagia
19	86	M	CBD	3	3 yr	n.d.	PSP
20	48	M	Unremarkable	0	(–)	(–)	Unremarkable

Abbreviations: CDR, clinical dementia rating (26) before suffering from terminal illness; PA, duration of Parkinsonism; Dementia, duration of dementia; yr, year; n.d., duration not determined due to unclear onset; PD, Parkinson disease; AD, Alzheimer disease; DLB, dementia with Lewy bodies; DLBN, DLB neocortical form (diffuse Lewy body disease); DLBT, DLB transitional form (limbic form); FTD, fronto-temporal dementia; MCI, mild cognitive impairment; CBD, corticobasal degeneration; CVD, cerebrovascular disease; N/A, not available; NFTD, neurofibrillary tangle-predominant form of dementia; CS, cervical spondylotic myelopathy; CVD, cerebrovascular disease; DG, dementia with grains; PSP, progressive supranuclear palsy; VD, vascular dementia of Binswanger type.

immunohistochemistry. Lewy dots outnumbered Lewy threads, making it unlikely that Lewy dots were simply cross sections of Lewy threads. The functional significance of these psyn-positive structures is open to speculation. Lewy dots and threads accompanied the cortical spongiosis associated with DLB, raising the possibility that they may disrupt synaptic transmission. The anti-psyn-immunoreactive axons in the affected limbic system suggest a possible disruption of axonal transport in LB-related cognitive decline. The presence of psyn-positive structures in the molecular layer of the occipital cortex in DLB neocortical form suggests a cause for the decreased uptake noted in occipital cortex with single photon emission computed tomography (SPECT) and fluordeoxy-glucose positron emission tomography (PET) studies of DLB (19, 20).

Our study confirmed that α-synucleinopathy may start in the medulla oblongata, as previously reported by Del Tredici (9). However, in 5 of 15 AD cases, the process appeared to start in the amygdala at Stage 0.5 and then progressed to mildly involve the brainstem in Stage II. These findings suggest that there are 2 types of LB-related α-synucleinopathy: a primary type that starts in the medulla oblongata, and a secondary type that starts in the amygdala. The primary type appears to progress into Parkinson disease and then DLB transitional form. The secondary type is associated with AD and possibly other tauopathies (21, 22), as was suggested by the association of one of our cases with PSP. The relation between DLB neocortical form and these primary and secondary types of α-synucleinopathy remains to be clarified.

Neostriatal pathology was reported with allosteric form-specific anti-α-synuclein antibody (23) and was confirmed by our anti-psyn immunocytochemistry. We observed numerous Lewy dots in a ventrolateral to dorsomedial gradient, consistent with the progression of Parkinson disease reported in a dopamine PET and biochemical study (24). The epitope of psyn was colocalized within plaques in dystrophic neurites or cores exclusively in some cases above Stage II. The possible association of Aβ and psyn deserves further study.

Our study showed that the neuropil pathology visualized with anti-psyn antibody was more widespread than reported previously. The observation that the presence of LBs was always accompanied by abundant neuropil pathology in the background supports the validity of the diagnostic criteria of DLB based on the LB score adopted

TABLE 2B
Neuropathological Summary of the Cases with Phosphorylated α-Synuclein-Related Neuronal Degeneration

Case	Stage	Score	tENT	Ci	F	T	P	O	NFT	SP
1	V	10 (10)	2 (2)	2 (2)	2 (2)	2 (2)	2 (2)	1	III	C
2	V	10 (9)	2 (2)	2 (2)	2 (2)	2 (2)	2 (1)	1	III	C
3	V	10 (8)	2 (2)	2 (2)	2 (1)	2 (2)	2 (1)	1	II	B
4	V	10 (9)	2 (2)	2 (2)	2 (2)	2 (2)	2 (1)	1	I	B
5	IV	10 (7)	2 (2)	2 (2)	2 (1)	2 (2)	2 (0)	1	I	B
6	IV	10 (7)	2 (2)	2 (2)	2 (1)	2 (2)	2 (0)	2	IV	B
7	IV	10 (7)	2 (2)	2 (2)	2 (1)	2 (2)	2 (0)	1	I	B
8	IV	10 (6)	2 (2)	2 (2)	2 (0)	2 (2)	2 (0)	1	I	A
9	IV	10 (6)	2 (2)	2 (2)	2 (0)	2 (2)	2 (0)	1	I	A
10	III	10 (6)	2 (2)	2 (2)	2 (0)	2 (2)	2 (0)	0.5	III	0
11	III	10 (6)	2 (2)	2 (2)	2 (0)	2 (2)	2 (0)	0.5	I	0
12	IIN	8 (6)	2 (2)	2 (2)	1 (0)	2 (2)	1 (0)	0.5	I	B
13	IIN	10 (8)	2 (2)	2 (2)	2 (0)	2 (2)	2 (1)	1	I	C
14	IIN	9 (5)	2 (2)	2 (1)	1 (1)	2 (0)	2 (1)	0.5	V	C
15	IIN	8 (5)	2 (2)	2 (2)	1 (0)	2 (1)	1 (0)	0	I	B
16	IIN	9 (6)	2 (2)	2 (1)	1 (0)	2 (2)	2 (1)	0.5	III	B
17	IIL	6 (2)	2 (0)	2 (1)	0 (0)	2 (1)	0 (0)	0	V	C
18	IIL	5 (3)	2 (1)	1 (1)	0 (0)	2 (1)	0 (0)	0	III	B
19	IIL	5 (0)	2 (0)	1 (0)	0 (0)	2 (0)	0 (0)	0	III	0
20	IIL	4 (0)	2 (0)	1 (0)	0 (0)	1 (0)	0 (0)	0	I	0

Scoring for Lewy bodies (score, tENT, Ci, F, T, and P) was assessed in sections immunostained for phosphorylated α-synuclein (psyn), following the consensus guidelines for dementia with LBs (6). The score in parentheses was determined by H&E staining and ubiquitin immunostaining. The score for Lewy bodies in the occipital cortex was determined by immunostaining for phosphorylated α-synuclein. Scores 0, 1, and 2 followed the consensus guidelines for dementia with LBs (6); the score 0.5 indicated Lewy threads and dots without intraneuronal perikaryal inclusions.

Abbreviations: NFT, neurofibrillary tangles, Braak staging (27); SP, senile plaque, Braak staging (27); Stage, Lewy body stage; Score, Lewy body score following consensus guidelines for dementia with LBs (6); tENT, transentorhinal area; Ci, cingulate gyrus; F, frontal lobe; T, temporal lobe; P, parietal lobe; O, occipital lobe.

by the consensus guidelines (6). The presence of widespread neuropil pathology is also consistent with previous reports that a decline of choline acetyl transferase (ChAT) is linearly correlated with the number of cortical LBs in the temporal neocortex (25).

Anti-psyn immunocytochemistry was too sensitive for assessment of Lewy scores using traditional criteria, making it necessary for us to adopt revised criteria. In our study, neocortical involvement was definitely present in the medial temporal lobe in Parkinson disease, spread to the frontal lobe in DLB transitional form, and additionally involved the parietal and occipital lobes in DLB neocortical form. This progressive involvement of the neocortex suggests that a revision of the diagnostic guidelines for LB-related cognitive decline may be warranted.

ACKNOWLEDGMENT

We thank Dr. Yasuo Ihara (Department of Neuropathology, University of Tokyo) for the donation of antibody; Mr. Naoo Aikyo, Mrs. Mieko Yamazaki, and Mrs. Nobuko Naoi for the preparation of sections; and Dr. Kinuko Suzuki (Department of Pathology and Laboratory Medicine, University of North Carolina at Chapel Hill) for helpful discussions and comments, and Dr. Thomas W. Bouldin (Department of Pathology and Laboratory Medicine, University of North Carolina at Chapel Hill) for kindly editing the manuscript. This work was supported by grants in aid from the Tokyo Metropolitan Institute of Gerontology.

REFERENCES

1. Kuzuhara S, Mori H, Izumiyama N, Yoshimura M, Ihara Y. Lewy bodies are ubiquitinated. A light and electron microscopic immunocytochemical study. Acta Neuropathol (Berl) 1988;75:345–53
2. Spillantini MG, Schmidt ML, Lee VM, Trojanowski JQ, Jakes R, Goedert M. α-Synuclein in Lewy bodies. Nature 1997;388:839–40
3. Baba M, Nakajo S, Tu PH, et al. Aggregation of α-synuclein in Lewy bodies of sporadic Parkinson's disease and dementia with Lewy bodies. Am J Pathol 1998;152:879–84
4. Iwanaga K, Wakabayashi K, Yoshimoto M, et al. Lewy body-type degeneration in cardiac plexus in Parkinson's and incidental Lewy body diseases. Neurology 1999;52:1269–71
5. Jackson M, Lennox G, Balsitis M, Lowe J. Lewy body dysphagia. J Neurol Neurosurg Psychiatry 1995;58:756–58
6. McKeith IG, Galasko D, Kosaka K, et al. Consensus guidelines for the clinical and pathologic diagnosis of dementia with Lewy bodies (DLB): Report of the consortium on DLB international workshop. Neurology 1996;47:1113–24
7. Lennox GG, Lowe J. Dementia with Lewy bodies. In: Markesbery WR, ed. Neuropathology of dementing disorders. London: Arnold, 1998:181–92
8. Esiri MM, McShane RH. Parkinson's disease and dementia. In: Esiri MM, Morris JH, eds. The neuropathology of dementia. Cambridge: Cambridge University Press, 1997:174–93

9. Del Tredici K, Rub U, De Vos RA, Bohl JR, Braak H. Where does Parkinson disease pathology begin in the brain? J Neuropathol Exp Neurol 2002;61:413–26
10. Lippa CF, Fujiwara H, Mann DM, et al. Lewy bodies contain altered α-synuclein in brains of many familial Alzheimer's disease patients with mutations in presenilin and amyloid precursor protein genes. Am J Pathol 1998;153:1365–70
11. Arai Y, Yamazaki M, Mori O, Muramatsu H, Asano G, Katayama Y. α-Synuclein-positive structures in cases with sporadic Alzheimer's disease: Morphology and its relationship to tau aggregation. Brain Res 2001;888:287–96
12. Jakes R, Spillantini MG, Goedert M. Identification of two distinct synucleins from human brain. FEBS Lett 1994;345:27–32
13. Fujiwara H, Hasegawa M, Dohmae N, et al. α-Synuclein is phosphorylated in synucleinopathy lesions. Nat Cell Biol 2002;4:160–64
14. Saito Y, Nakahara K, Yamanouchi H, Murayama S. Severe involvement of ambient gyrus in dementia with grains. J Neuropath Exp Neurol 2002;61:789–96
15. McKeith IG, Perry EK, Perry RH. Report of the second dementia with Lewy body international workshop: Diagnosis and treatment. Consortium on Dementia with Lewy Bodies. Neurology 1999;53: 902–5
16. Hasegawa M, Fujiwara H, Nonaka T, et al. Phosphorylated α-synuclein is ubiquitinated in α-synucleinopathy lesions. J Biol Chem 2002;277:49071–76
17. Kato T, Hirano A, Weinberg MN, Jacobs AK. Spinal cord lesions in progressive supranuclear palsy: Some new observations. Acta Neuropathol (Berl) 1986;71:11–14
18. Braak H, Braak E. Argyrophilic grains: Characteristic pathology of cerebral cortex in cases of adult onset dementia without Alzheimer changes. Neurosci Lett 1987;76:124–27
19. Ishii K, Yamaji S, Kitagaki H, Imamura T, Hirono N, Mori E. Regional cerebral blood flow difference between dementia with Lewy bodies and AD. Neurology 1999;53:413–16
20. Imamura T, Ishii K, Sasaki M, et al. Regional cerebral glucose metabolism in dementia with Lewy bodies and Alzheimer's disease: A comparative study using positron emission tomography. Neurosci Lett 1997;235:49–52
21. Forman MS, Schmidt ML, Kasturi S, Perl DP, Lee VM, Trojanowski JQ. Tau and α-synuclein pathology in amygdala of Parkinsonism-dementia complex patients of Guam. Am J Pathol 2002; 160:1725–31
22. Saito Y, Kawai M, Inoue K, et al. Widespread expression of α-synuclein and tau immunoreactivity in Hallervorden-Spatz syndrome with protracted clinical course. J Neurol Sci 2000;177:48–59
23. Duda JE, Giasson BI, Mabon ME, Lee VMY, Trojanowski JQ. Novel antibodies to synuclein show abundant striatal pathology in Lewy body disease. Ann Neurol 2002;52:205–10
24. Piggott MA, Marshall EF, Thomas N, et al. Striatal dopaminergic markers in dementia with Lewy bodies, Alzheimer's and Parkinson's diseases: Rostrocaudal distribution. Brain 1999;123:1449–68
25. Perry EK, Haroutunian V, Davis KL, et al. Neocortical cholinergic activities differentiate Lewy body dementia from classical Alzheimer's disease. Neuroreport 1994;5:747–49
26. Hughes CP, Berg L, Danziger WL, Coben LA, Martin RL. A new clinical scale for the staging of dementia. Br J Psychiatry 1982; 140:566–72
27. Braak H, Braak E. Neuropathological stageing of Alzheimer-related changes. Acta Neuropathol (Berl) 1991;82:339–59

Received October 25, 2002
Revision received January 22, 2003
Accepted February 11, 2003

Journal of Neuropathology and Experimental Neurology

Vol. 61, No. 9
September, 2002
pp. 789–796

Severe Involvement of Ambient Gyrus in Dementia with Grains

YUKO SAITO, MD, PHD, KENICHI NAKAHARA, MD, PHD, HIROSHI YAMANOUCHI, MD, PHD, AND SHIGEO MURAYAMA, MD, PHD

Abstract. Argyrophilic grains are detected as punctate or filiform structures in the neuropil of the medial temporal lobe, and dementia with grains (DG) is defined as a form of dementia with argyrophilic grains as the only explainable cause. We found argyrophilic grains in 43.2% of our 190 serial autopsy brains (mean age, 79.7 yr) from a community-based geriatric hospital, but only 20% of these argyrophilic grain-positive brains fulfilled the criteria for DG. To determine if there are structural differences between cognitively normal cases with argyrophilic grains (CNG) and DG, we studied 14 brains with CNG and 15 brains with DG. All cases of DG had severe atrophy of the ambient gyrus (the junction between temporal lobe and amygdala) with spongiosis, neuronal loss, and gliosis, as well as many grains, pretangles, coiled bodies, and tau-immunoreactive astrocytes. Comparable changes were not present in the ambient gyrus of CNG brains. The temporal neocortex and hippocampus were relatively spared in DG, in contrast to Alzheimer disease. Our study suggests that selective severe involvement of the ambient gyrus may explain the clinical manifestations of a limbic-type dementia in DG.

Key Words: Aging; Dementia with grains: Immunocytochemistry; Senile dementia; Tau; Tauopathy.

INTRODUCTION

Argyrophilic grains are punctate or filiform structures in the neuropil and are best demonstrated with Gallyas-Braak (G-B) silver staining (1). Argyrophilic grains are most abundant in the CA1 subfield of hippocampus, the entorhinal and transentorhinal cortex and adjacent temporal isocortex, the amygdala, the hypothalamic lateral tuberal nuclei, the rectus gyrus, and the septal nuclei (2). Argyrophilic grain dementia or dementia with grains (DG) is defined by Braak and Braak (2, 3) as a form of senile dementia that has only argyrophilic grains as a morphological cause of dementia. In their series of 56 brains from patients with adult-onset dementia and no cerebrovascular disease, 8 had argyrophilic grains, 8 had argyrophilic grains with changes of Alzheimer disease (AD), and 40 had AD (3). Argyrophilic grains are immunoreactive with anti-tau antibodies (4–6), and DG may be classified as a form of tauopathy.

Argyrophilic grains are also reported in cognitively normal subjects (7–9) and in a large variety of neurodegenerative disorders in the aged population, including AD, progressive supranuclear palsy, corticobasal degeneration, dementia with Lewy bodies, Pick disease, multiple system atrophy, Parkinson disease, amyotrophic lateral sclerosis, and the neurofibrillary tangle-predominant form of dementia (4, 8, 10, 11). The term *argyrophilic grain disease* has been applied to brains with abundant argyrophilic grains, and the term *DG* to the subgroup of patients with argyrophilic grain disease and a definite clinical history of dementia (9, 12).

Multiple studies support the independence of DG from AD. These data include 1) a higher frequency of the ε2 genotype of apolipoprotein E (apoE) (13, 14) in DG than AD; 2) the constant finding of αB-crystallin-positive ballooned neurons in the amygdala in DG (15); 3) the presence of abundant tau-immunoreactive astrocytes in DG (16); and 4) the preferential deposition of neocortical diffuse plaques rather than neuritic plaques in DG (17). Despite these genotypic and immunohistochemical differences, the clinical presentation of DG largely overlaps that of AD, such that the clinical distinction between the two is difficult (18).

We recently performed G-B staining and tau immunocytochemistry on brains from serial autopsy cases in our institute and found a relatively high frequency of argyrophilic grains in these brains. However, only a small percentage of the argyrophilic grain-positive cases fulfilled the clinical and pathological criteria for DG. Further analysis of the brains containing argyrophilic grains revealed that severe involvement of the ambient gyrus was limited to brains showing both argyrophilic grains and a clinical history of dementia. The purposes of the current study are to establish the significance of ambient gyrus degeneration in DG and to document the relative frequency of DG among dementing disorders in the aged population.

MATERIALS AND METHODS

Cases

One hundred and ninety postmortem brains submitted for morphological examination in our department from June 1999 to May 2000 were the basis of the present work. The brains were from consecutive autopsy cases that included permission for brain examination at Tokyo Metropolitan Geriatric Hospital, an institution that provides community-based medical services

From the Department of Neuropathology (YS, SM), Tokyo Metropolitan Institute of Gerontology, Tokyo, Japan; Departments of Laboratory Medicine (KN) and Neurology (HY), Tokyo Metropolitan Geriatric Hospital, Tokyo, Japan.

Correspondence to: Shigeo Murayama, MD, PhD, Department of Neuropathology, Tokyo Metropolitan Institute of Gerontology, 35-2Sakaecho, Itabashi-ku, Tokyo 173-0015, Japan.

TABLE 1
Case Profile of Argyrophilic Grain Disease with Dementia (DG)

a. Clinical profiles of dementia with grains

Case	Age	Gender	CDR	ApoE	MMSE	HDS-R	Interval (yr)	CC (yr)
1	78	M	1	3/3	21/30		0.5	>1
2	80	M	1	2/3	19/30		0.2	>1
3	81	M	2	3/3	9/30		3	9
4	84	M	1	3/3	18/30		1	>1
5	86	M	1	3/3	N/A		1.5	>1
6	86	M	3	2/3		5/30	1	7
7	91	M	1	3/3	N/A		1	>1
8	82	F	1	3/3	N/A		0.5	>1
9	83	F	1	2/3	25/30		2	>1
10	86	F	3	3/3	0/30		1	23
11	88	F	2	3/3	2/30		0.2	>0.2
12	89	F	1	3/3	0/30		9	20
13	91	F	3	2/3	0/30		0.5	14
14	96	F	3	2/3	0/30		8	8
15	98	F	3	3/3	0/30		5	9

b. Pathological profiles

			Lewy body			Grains					Deg.
Case	BW (g)	NFT	SP	B-S & Am	Cortex	AA	AmG	pSub	mTp	aCg	AmG
1	1340	II	B	0	0	1	3	3	1	1	+
2	1240	II	B	0	0	0	3	3	2	2	++
3	1265	I	A	0	0	0	3	3	1	1	++
4	1220	I	B	0	0	0	3	3	2	1	+
5	1270	I	A	0	0	0	3	3	1	1	+
6	1150	I	A	i	0	0	3	3	1	1	+
7	1240	I	A	0	0	0	3	3	1	1	++
8	1280	I	A	0	0	0	3	3	1	1	+
9	990	I	A	0	0	0	3	3	1	1	+
10	1250	II	A	i	1	1	3	3	2	1	++
11	1170	II	B	0	0	1	3	3	1	1	+
12	1200	II	A	i	0	0	3	3	1	1	+
13	1050	II	B	0	0	0	3	3	2	2	+++
14	1390	I	A	i	1	0	3	3	2	2	+++
15	1140	I	B	i	1	0	3	3	1	1	++

Abbreviations: CDR, clinical dementia rating before suffering from the last fatal illness; ApoE, apolipoprotein E; MMSE, mini mental state examination; HDS-R, Hasegawa dementia scale revised; Interval, the interval between the last mental examination and death; N/A, not available due to the patient's refusal; BW, brain weight; NFT, neurofibrillary tangles, Braak staging (42); SP, senile plaques, Braak staging (42); AG, argyrophilic grains; AA, amyloid angiopathy; CC, clinical course of dementia documented by medical staff; B-S & Am, brainstem and amygdala; Cortex, cerebral cortex; Deg., degeneration; Amg, ambient gyrus; pSub, posterior subiculum; mTp, medial temporal pole; aCg, anterior cingulate gyrus.

Scoring for Lewy body is as follows: 0 = none; i = a few Lewy bodies without neuronal degeneration; 1 = following diagnostic rating protocol by Consensus Guidelines for Dementia with Lewy bodies (32). Scoring for AA is as follows: 0 = none; 1 = mild; 2 = moderate with degenerative changes in the arterial walls; and 3 = severe with hemorrhage. Scoring of argyrophilic grains is based on number of grains in a ×400 field as follows: 1 = 20–50 grains; 2 = 50–100 grains; and 3 = >100 grains. Scoring for degeneration: + = mild (gliosis is only detectable by GFAP immunostaining); ++ = moderate (gliosis is easily seen with H&E stain); and +++ = severe (neuronal loss with rarefaction of the tissue is prominent).

to the aged. The patients' ages ranged from 60 to 103 yr, with a mean of 79.7 yr and a male to female ratio of 106:84.

Clinical Features

Clinical information was obtained from medical charts and from interviews with relevant physicians and caregivers. The Mini-Mental State Examination (MMSE) (19) or the Hasegawa dementia scale (20, 21) were used for evaluation of cognitive function and the clinical dementia rating scale (CDR) (22) was used for grading of dementia. The Hasegawa dementia scale is a screening tool for cognitive decline in the elderly and has the same sensitivity and specificity as the MMSE (21).

Neuropathology

Routine Pathology: The right medial temporal lobe was resected at the time of autopsy and divided into 3 portions. The 3 portions were placed in 4% paraformaldehyde fixative for histochemical and immunocytochemical studies, half-strength Karnovsky fixative for electron microscopy, and liquid nitrogen for snap-freezing for biochemical and molecular pathology studies, respectively. The remainder of the brain was fixed in 20% buffered formalin for further morphological study. Multiple areas from the formalin-fixed brain were embedded in paraffin, serially sectioned at 6-μm, and stained with hematoxylin and eosin (H&E) and Klüver-Barrera. Areas examined included bilateral temporal poles, amygdala at the level of ambient gyrus, anterior and posterior hippocampus with entorhinal and transentorhinal areas, left rectal gyrus and septal area, the left frontal, temporal, parietal, and cingulate cortex as recommended by CERAD (23). Also sampled were the left primary motor area, visual cortex, basal ganglia at the level of mamillary body, thalamus at the level of red nucleus, subthalamic nucleus, hypothalamus, midbrain, upper and middle pons, medulla oblongata, cerebellar vermis, dentate nucleus, and the cervical, thoracic, and lumbar spinal cord. Selected sections were stained with Congo red and various silver stains, including Gallyas-Braak (G-B) (24), modified methenamine silver (MMS) (25), Bielschowsky, and Bodian methods.

Immunocytochemistry: The various anti-tau antibodies employed and their epitopes were as follows: AT8, phosphorylated Ser-202/Thr-205 (monoclonal; Innogenetics, Temse, Belgium); AP422, phosphorylated Ser-422 (polyclonal; a gift from Dr. Y. Ihara); Alz50, amino acids 5–51, 312–322 (monoclonal; a gift from Dr. P. Davies); and PHF1, Ser-396/404, (monoclonal; a gift from Dr. P. Davies). Also employed were antibodies raised against glial fibrillary acidic protein (GFAP) (polyclonal; Dako, Carpinteria, CA); HLA-DR (CD68, Dako); Aβ 1–42 (polyclonal, IBL, Maebashi, Japan); Aβ11–28 (12B2, IBL); α-synuclein (LB509; a gift from Dr T. Iwatsubo); αB-crystallin (polyclonal; a gift from Dr. H. Mori) and ubiquitin (polyclonal; Dako).

TABLE 2
Case Profiles of Argyrophilic Grain Disease without Dementia (CNG)

Case	Age	Gender	CDR	ApoE	BW (g)	NFT	SP	Grains*		LB**	AA	Deg. AmG
								AmG	pSub			
1	68	M	0	3/4	1410	I	A	1	0	0	0	−
2	72	M	0	3/4	1370	I	B	1	0	0	0	−
3	72	M	0	3/3	1360	I	A	2	1	0	1	+/−
4	75	M	0	3/3	1490	I	B	1	0	0	0	−
5	75	M	0	3/3	1055	0	B	2	1	0	0	+/−
6	76	M	0	3/3	1450	I	B	1	0	0	0	−
7	80	M	0	3/3	1120	I	0	1	0	0	0	−
8	83	M	0	3/3	1280	I	A	3	2	i	1	+/−
9	75	F	0	3/3	1135	I	B	1	0	0	0	−
10	75	F	0	3/3	1200	I	0	2	1	0	1	+/−
11	79	F	0	3/3	1160	I	A	1	0	i	0	−
12	80	F	0	2/3	1270	I	B	1	0	0	0	−
13	82	F	0	3/3	1220	II	A	2	1	0	0	+/−
14	84	F	0	3/3	1160	I	B	3	2	0	0	+/−

Abbreviations for Table 2 are the same as for Table 1, except that scoring of degeneration of ambient gyrus (Deg. AmG) is as follows: − = no tau-immunoreactive astrocytes; +/− = less than 5 tau-immunoreactive Gallyas-negative astrocytes in a section of the ambient.

* No grains found in medial temporal pole or anterior cingulate gyrus in these CNG cases.

** LB = Lewy bodies in brainstem and amygdala. No Lewy body is observed in the cerebral cortex in these cases.

Serial 6-μm-thick sections of right and left temporal pole, ambient gyrus, anterior and posterior hippocampus, and midbrain were prepared for immunocytochemical study. Sections were pretreated by heating in a microwave oven for the anti-ubiquitin antibody and LB509, and by incubation with formic acid for anti-Aβ1–42 and Aβ 11–28 antibodies, as previously reported (26). The sections were then processed using an automatic immunostaining apparatus for single or double immunostaining (27, 28) (Ventana NX20; Ventana, Tucson, AZ).

Molecular Pathological Study: Genomic DNA was extracted from the kidney, which was snap-frozen at autopsy, and apoE genotyping was determined by PCR (29). There were 1,107 of 1,227 serial autopsy cases starting January 27, 1995 examined, including 181 of the 190 cases in the present series. Genotypes and allelic frequencies were statistically analyzed by χ^2 test or the Fisher exact test, with $p < 0.01$ interpreted as significant.

Diagnostic Criteria of Each Type of Dementia

The diagnosis of DG was based on Jellinger's definition (30): 1) widespread occurrence of minute, spindle- or comma-shaped, argyrophilic tau-immunoreactive structures distinct from neuropil threads and predominantly located in the hippocampus and related limbic areas, including the amygdala; 2) accompanying clinical evidence of dementia; and 3) absence of other morphological causes of dementia. The diagnosis of the neurofibrillary tangle-predominant form of dementia was also based on Jellinger's definition (10) and includes the following: 1) tangles restricted to hippocampus, entorhinal and transentorhinal areas and fitting Braak tangle stage III or IV; 2) the frequency of tangles being extensive and usually greater than that seen in AD; and 3) the frequency of senile plaques being the same or less than that found in normal age-matched controls. NIA-Regan criteria (31) and consortium criteria (32) were adopted for the diagnosis of AD and dementia with Lewy bodies, respectively. The diagnosis of vascular dementia was based on the State of California AD Diagnostic and Treatment Centers criteria (the "California criteria") (33) and/or the National Institute of Neurologic Disorders and Stroke and the Association Internationale pour la Recherche et l'Enseignement en Neurosciences (NINDS-AIREN) criteria (34).

Selection of DG and CNG

Fifteen pure DG cases were identified after employing the following neuropathological exclusion criteria: 1) presence of plaque staging of Braak C; 2) presence of tangle staging of more than Braak III; 3) presence of prominent amyloid angiopathy; or 4) presence of major vascular pathology. Fourteen CNG cases were identified. These 14 cases had none of the exclusionary neuropathological findings and had definite evidence of normal cognitive function until the last admission, as documented by the clinical charts and by the attending physicians, nurses, and caregivers.

RESULTS

Relative Frequency of DG among Demented Population

One hundred and one of the 190 autopsied cases (53.2%) had clinically documented dementia. The brains from these demented cases were pathologically classified as follows: 28 cases of vascular dementia, 52 cases of degenerative dementia, 3 cases of mixed dementia, and 18 cases of other causes. The 52 cases of degenerative dementia included 22 cases of AD, 15 cases of DG, 6 cases of dementia with Lewy bodies, 2 cases of neurofibrillary tangle-predominant form of dementia, 1 case of

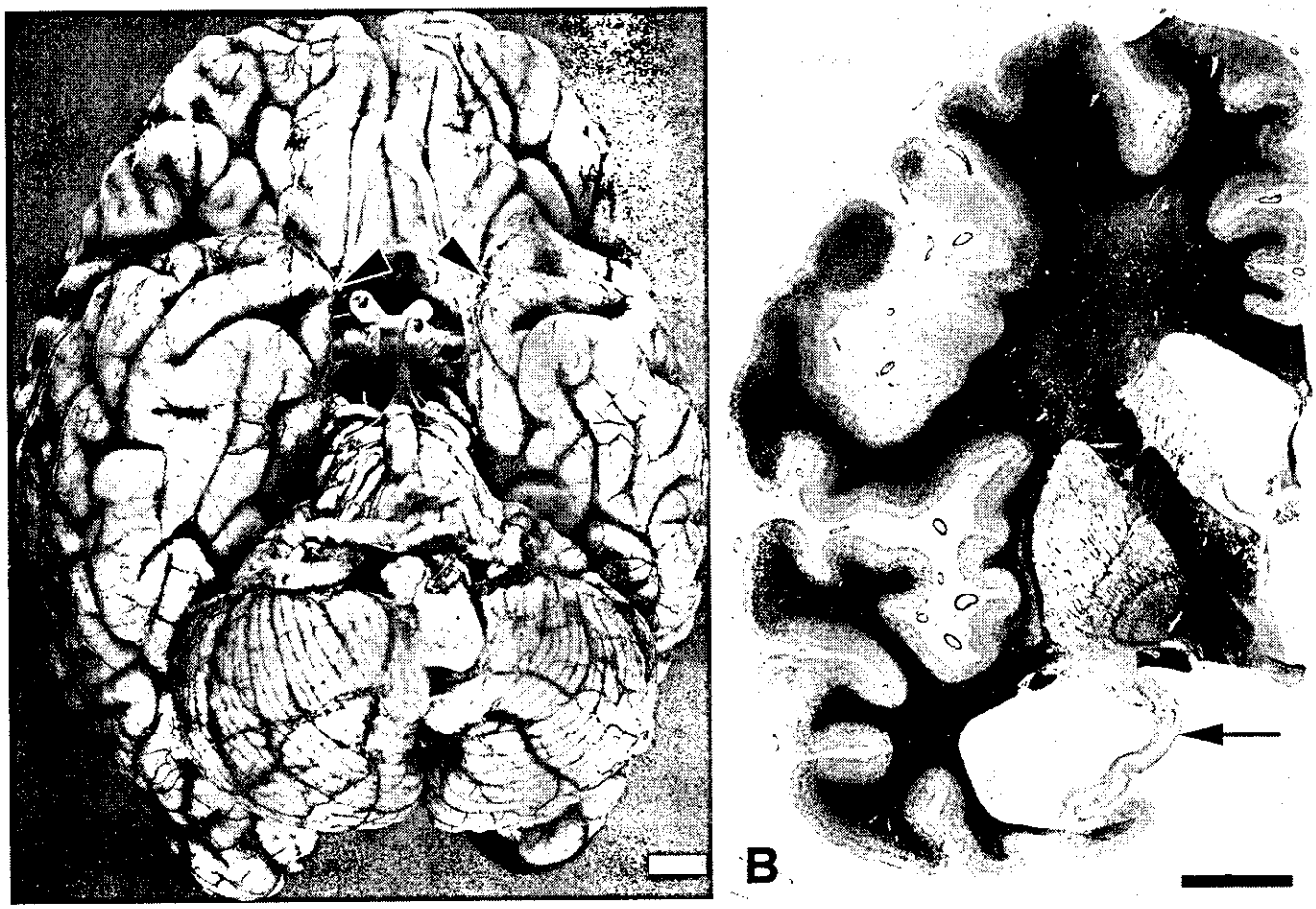

Fig. 1. Severe atrophy of ambient gyrus in a case of dementia with grains (Case 14). A: Inferior surface of unfixed brain showing the anterior medial temporal lobe with accentuation of atrophy in the ambient gyrus (arrowheads). B: Coronal hemispheric section at level of mamillary body demonstrates marked atrophy of the ambient gyrus (arrow) and sparing of the temporal and frontal neocortex (Klüver-Barrera stain). Scale bar: A, B = 1 cm.

progressive supranuclear palsy, 4 cases of AD plus dementia with Lewy bodies, 1 case of DG plus dementia with Lewy bodies, and 1 case of DG plus progressive supranuclear palsy.

Argyrophilic grains were seen in 81 of the 190 cases (42.6%). Forty-seven (46.5%) of the 101 cases with dementia had argyrophilic grains, and 34 (38.2%) of the 89 cases without dementia had grains. The age distribution of argyrophilic grains was as follows: 60 to 69 yr, 3 of 14 cases (21.4%); 70 to 79 yr, 26 of 73 cases (35.6%); 80 to 89 yr, 38 of 74 cases (51.4%); 90 to 99 yr, 14 of 28 cases (50%); and 100 to 103 yr, 0 of 1 case.

Comparative Study of Brains with DG and CNG

The profiles of the DG and the CNG cases are summarized in Tables 1 and 2. The DG cases included 7 males and 8 females, with ages ranging from 79 to 98 yr (mean age, 86.5 yr) and brain weights ranging from 990 g to 1,390 g (mean weight, 1,212 g). Five DG cases (cases 3, 5, and 7–9) were almost free of other senile changes. By comparison, the CNG cases included 8 male and 6 female, with ages ranging from 68 to 84 yr (mean age, 76.4 yr) and brain weights ranging from 1,055 g to 1,490 g (mean weight, 1,263 g).

Macroscopically, the DG brains showed atrophy of the medial temporal lobe, whereas the CNG cases had no significant abnormalities. The temporal lobe atrophy in the DG brains was greater anteriorly and was accentuated at the junction between temporal lobe and amygdala, such that the ambient gyrus (35–37) was constantly involved (Fig. 1A, B). The posterior hippocampus and entorhinal areas were relatively spared.

Microscopically, the distribution of argyrophilic grains was much more restricted in the CNG brains than in the DG brains. In 8 of 14 CNG cases, argyrophilic grains were limited to the ambient gyrus and anterior CA1 area, with accompanying oligodendroglial coiled bodies in the subcortical white matter. In the remaining 6 cases the argyrophilic grains had a wider distribution, extending to the posterior CA1, subiculum and transentorhinal area, and the basal and lateral subnuclei of the amygdala. Also present in these latter 6 cases of CNG were pretangles in

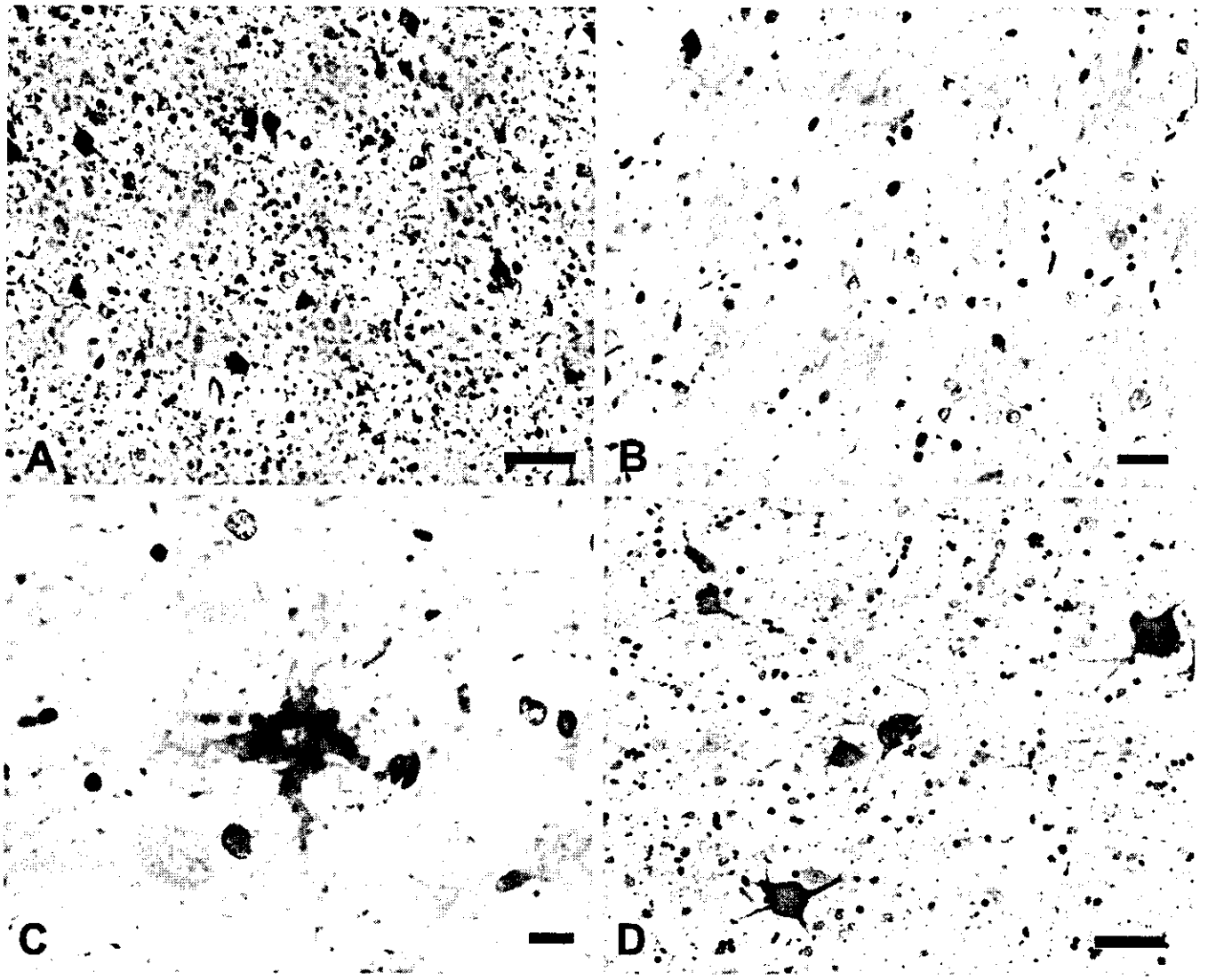

Fig. 2. Histopathological features of dementia with grains. A: Abundant argyrophilic grains are visualized immunocytochemically with anti-phosphorylated tau antibody (case 8, transentorhinal area, AT8-immunostaining. B: Spongiosis is associated with argyrophilic grains in the ambient gyrus (case 8, Gallyas-Braak silver stain). C: Double immunostaining with AT8 (brown) and anti-glial fibrillary acidic protein antibody (red) demonstrates a gemistocytic astrocyte with focal tau-immunoreactivity. D: Double immunostaining with AT8 (brown) and anti-αB-crystallin antibody (red) reveals tau-immunoreactivity in the periphery and αB-crystallin-immunoreactivity in the center of ballooned neurons. Scale bars: A, B = 50 μm; C = 10 μm; D = 100 μm.

the dentate gyrus and hippocampal CA2 subfield, tau-immunoreactive astrocytes (16) preferentially present around the uncal horn and in the amygdala, and rare ballooned neurons in the basal and lateral subnuclei of the amygdala. In contrast, the DG brains uniformly showed a much wider distribution of argyrophilic grains (Fig. 2A), with grains extending as far as the medial side of the temporal pole (Fig. 3).

Another distinctive histopathological difference between the DG and CNG cases was the presence of a superficial spongiosis associated with the argyrophilic grains (Fig. 2B) in the DG brains. The spongiosis was most prominent in the ambient gyrus, but was also present in the cortical subnuclei of the amygdala, in the entorhinal and transentorhinal areas, and in the subiculum. As the spongiosis became more severe, the argyrophilic grains became less numerous. A reactive tau-immunopositive astrocytosis, best demonstrated by double immunostaining with AT8 and GFAP (Fig. 2C), always accompanied the spongiosis. The CNG brains had only scattered AT8-immunoreactive astrocytes in the middle layer of the ambient gyrus in some cases (Table 2).

Pathological changes in the dentate gyrus, a predilection site for pretangles (38), showed some overlap between DG and CNG cases. The DG brains had abundant numbers of AT8-immunoreactive pretangles but no grains in dentate gyrus, as previously reported (38). Eight of the CNG brains (CNG cases 1, 2, 4, 6, 7, 9, 11 and 12) had

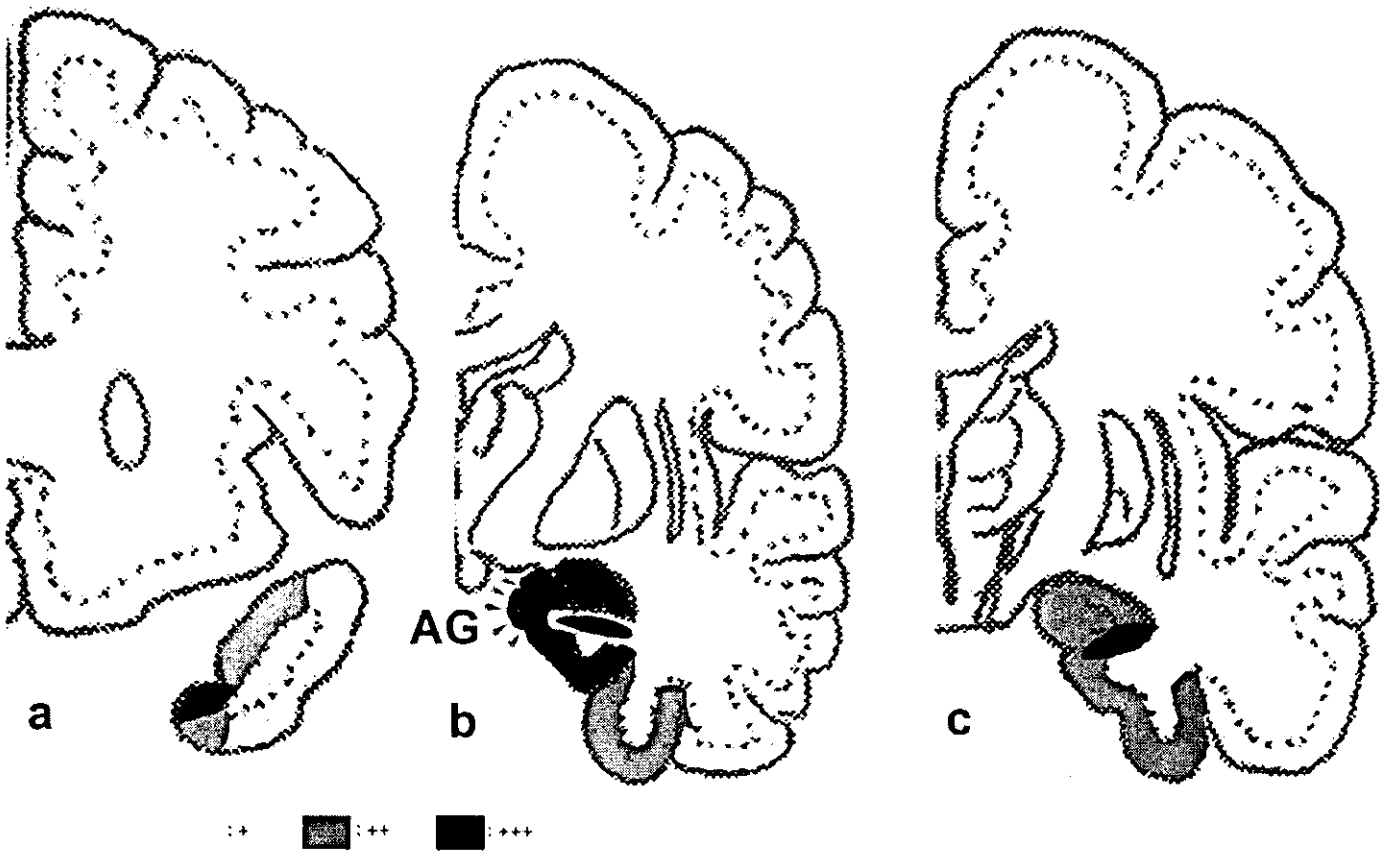

Fig. 3. The topographical distribution and frequency of argyrophilic grains in cases of dementia with grains. The 3 coronal brain sections are from the level of the genu of corpus callosum (a), the mammillary body (b), and the lateral geniculate body (c). Scoring of the frequency of argyrophilic grains in GB-stained sections is based on the number of grains in a ×400 field as follows: + = 20–50; ++ = 50–100; and +++ = >100. Arrowheads indicate the ambient gyrus (AG).

no pretangles, 4 (CNG cases 3, 5, 10 and 13) had rare pretangles, and 2 (CNG cases 8 and 14) had numbers of pretangles comparable to those in DG brains.

Tau-immunoreactive ballooned neurons and coiled bodies were usually associated with grains. Ballooned neurons were most frequent in the basal and lateral subnuclei of amygdala, and coiled bodies were most frequent in the subcortical white matter of the affected area. Double immunostaining with AT8 and anti-αB-crystallin antibody showed peripheral localization of the AT8-immunoreactivity and central accumulation of the αB-crystallin epitope (Fig. 2D). AT8-immunoreactive granulovacuolar degeneration (39) was frequently seen in the areas abundant with grains and often associated with swollen neurons.

ApoE Genotyping

The results of apoE genotyping are summarized in Table 3. The genotype distributions and allele frequencies between the DG cases and the background were significantly different (χ^2 = 14.4 and 14.5, $p < 0.005$ and $p < 0.001$, respectively). The frequency of ε2 allele in the DG cases was significantly increased when compared with the background (26.7% vs 3.9%, $p < 0.01$ [Fisher exact test]) and with the AD cases (16.7% vs 0%, $p < 0.01$ [Fisher exact test]), but not when compared with the CNG cases (16.7% vs 3.6%, $p = 0.195$ [Fisher exact test]). In contrast, the frequency of ε4 allele in the DG cases was significantly decreased compared with the AD cases (0% vs 27.3%, $p < 0.005$ [Fisher exact test]). There was no significant difference in distribution of genotypes or frequencies of alleles between cases with and without argyrophilic grains (χ^2 = 3.9 and 3.6, $p = 0.27$, and $p = 0.16$, respectively).

DISCUSSION

Our postmortem examination of the brains from 190 serial autopsies at a geriatric hospital revealed that the incidence of argyrophilic grains increased with age and peaked at 50% in subjects over 80-yr-old. The argyrophilic grains were limited to the medial temporal lobe, with the ambient gyrus being preferentially involved. Thus, argyrophilic grains are an age-related morphological change, like neurofibrillary tangles and senile plaques, and have a unique and highly restricted topographical distribution in the brain.

TABLE 3
Frequency of Apolipoprotein E (apoE) Genotyping in Dementia with Grains (DG) and Control Cases

	DG	CNG	AD	With grains	Without grains	Background
n	15	14	22	81	109	1107
Genotypes						
ε2/ε3	5 (33.3%)	1 (7.1%)	0	11 (13.6%)	9 (8.2%)	86 (7.8%)
ε3/ε3	10 (66.7%)	11 (78.6%)	13 (59.1%)	57 (70.4%)	76 (69.7%)	846 (76.4%)
ε3/ε4	0	2 (14.3%)	6 (27.3%)	9 (11.1%)	16 (14.7%)	160 (14.5%)
ε4/ε4	0	0	3 (13.6%)	0	3 (2.8%)	15 (1.3%)
N/A	0	0	0	4 (4.9%)	5 (4.6%)	0
Alleles						
ε2	5 (16.7%)	1 (3.6%)	0	11 (6.8%)	9 (4.1%)	86 (3.9%)
ε3	25 (83.3%)	25 (89.3%)	32 (72.7%)	134 (82.7%)	177 (81.2%)	1938 (87.5%)
ε4	0	2 (7.1%)	12 (27.3%)	9 (5.6%)	22 (10.1%)	190 (8.6%)
N/A	0	0	0	8 (4.9%)	10 (4.6%)	0

Abbreviations: DG: dementia with grains; CNG: argyrophilic grain disease without cognitive impairment; AD: Alzheimer disease. Significant differences were detected between DG and AD and between DG and background for the ε2 allele, and between DG and AD for the ε4 allele.

Of the 52 cases of degenerative dementia in our serial autopsy study, 22 were classified as AD and 15 as DG. DG was thus the second most common cause of degenerative dementia in our series. Other investigators have also reported a similar ratio of DG to AD cases in a large autopsy series (38).

We previously reported severe atrophy of the ambient gyrus in a case of DG (40). Our current study of 15 additional cases of DG confirms the constant degeneration of the ambient gyrus and adjacent medial temporal lobe in DG. The atrophy is characterized microscopically by a grain-associated spongiosis, neuronal loss, and gliosis. Brains with argyrophilic grains from cognitively normal individuals had neither grain-associated spongiosis nor atrophy of the ambient gyrus. From these observations, we conclude that the degeneration of the ambient gyrus is the morphological substrate of the dementia in DG.

The ambient gyrus is the anterior part of subiculum, forming the junction between the amygdala and the temporal lobe. The ambient gyrus is an important part of the limbic loop, which is proposed to play an important role in the clinical presentation of dementia in many neurodegenerative disorders (41). This preferential involvement of the junctional region between the temporal lobe and amygdala may explain some of the reported clinical manifestations of DG, such as aggressiveness and ill-temper (18).

The preferential accumulation of the ε2 allele and absence of the ε4 allele of apoE in DG is consistent with previously reported genotypic analyses and contrasts with the preferential accumulation of the ε4 allele in AD (13, 14). These genotypic data underscore the distinctness of DG from AD. The data also suggest that the pathogenesis of argyrophilic grains is not influenced by apoE genotypes. We cannot find significant genotypic difference between CNG and DG in this study. Further studies, including the objective staging of the appearance of argyrophilic grains in a large series of autopsy cases with DG and CNG, may be important for determining the biological significance of argyrophilic grains and their role in the pathogenesis of DG.

ACKNOWLEDGMENTS

The authors thank Drs. Peter Davies, Takeshi Iwatsubo, Hiroshi Mori and Yasuo Ihara for the donation of their antibodies; Mr. Naoo Aikyo, Ms. Masako Maeda, Ms. Mieko Yamazaki, Ms. Sachiko Sugiura, Ms. Chieko Kanai, Ms. Hiroko Matsuoka and Mr. Yoshihiro Fujita for technical support; Professor Kinuko Suzuki for encouraging and advising this study, and Professor Thomas W. Bouldin for editing the manuscript. This study was supported by grants-in-aid from Tokyo Metropolitan Institute of Gerontology. A part of this study was presented at the 76th Annual Meeting of the American Association of Neuropathologists Inc. held in Atlanta, Georgia, June 2000.

REFERENCES

1. Gallyas F. Silver staining of Alzheimer's neurofibrillary changes by means of physical development. Acta Morphol Acad Sci Hung 1971;19:1–8
2. Braak H, Braak E. Cortical and subcortical argyrophilic grains characterize a disease associated with adult onset dementia. Neuropathol Appl Neurobiol 1989;15:13–26
3. Braak H, Braak E. Argyrophilic grains: Characteristic pathology of cerebral cortex in cases of adult onset dementia without Alzheimer changes. Neurosci Lett 1987;76:124–27
4. Ikeda K, Akiyama H, Kondo H, Haga C. A study of dementia with argyrophilic grains. Possible cytoskeletal abnormality in dendrospinal portion of neurons and oligodendroglia. Acta Neuropathol 1995;89:409–14
5. Itagaki S, McGeer PL, Akiyama H, et al. A case of adult-onset dementia with argyrophilic grains. Ann Neurol 1989;26:685–89

6. Masliah E, Hansen LA, Quijada S, et al. Late onset dementia with argyrophilic grains and subcortical tangles or atypical progressive supranuclear palsy? Ann Neurol 1991;29:389–96
7. Braak E, Braak H, Mandelkow EM. A sequence of cytoskeleton changes related to the formation of neurofibrillary tangles and neuropil threads. Acta Neuropathol 1994;87:554–67
8. Martinez-Lage P, Munoz DG. Prevalence and disease associations of argyrophilic grains of Braak. J Neuropathol Exp Neurol 1997; 56:157–64
9. Tolnay M, Schwietert M, Monsch AU, Staehelin HB, Langui D, Probst A. Argyrophilic grain disease: Distribution of grains in patients with and without dementia. Acta Neuropathol (Berl) 1997; 94:353–58
10. Jellinger KA, Bancher C. Senile dementia with tangles (tangle predominant form of senile dementia). Brain Pathol 1998;8:367–76
11. Ulrich J, Spillantini MG, Goedert M, Dukas L, Staehelin HB. Abundant neurofibrillary tangles without senile plaques in a subset of patients with senile dementia. Neurodegeneration 1992;1:257–64
12. Tolnay M, Spillantini MG, Goedert M, Ulrich J, Langui D, Probst A. Argyrophilic grain disease: Widespread hyperphosphorylation of tau protein in limbic neurons. Acta Neuropathol (Berl) 1997;93: 477–84
13. Ghebremedhin E, Schultz C, Botez G, et al. Argyrophilic grain disease is associated with apolipoprotein E epsilon 2 allele. Acta Neuropathol (Berl) 1998;96:222–24
14. Tolnay M, Probst A, Monsch AU, Staehelin HB, Egensperger R. Apolipoprotein E allele frequencies in argyrophilic grain disease. Acta Neuropathol (Berl) 1998;96:225–27
15. Tolnay M, Probst A. Ballooned neurons expressing alphaB-crystallin as a constant feature of the amygdala in argyrophilic grain disease. Neurosci Lett 1998;246:165–68
16. Botez G, Probst A, Ipsen S, Tolnay M. Astrocytes expressing hyperphosphorylated tau protein without glial fibrillary tangles in argyrophilic grain disease. Acta Neuropathol (Berl) 1999;98:251–56
17. Tolnay M, Calhoun M, Pham HC, Egensperger R, Probst A. Low amyloid (Aβ) plaque load and relative predominance of diffuse plaques distinguish argyrophilic grain disease from Alzheimer's disease. Neuropathol Appl Neurobiol 1999;25:295–305
18. Ikeda K, Akiyama H, Arai T, Matsushita M, Tsuchiya K, Miyazaki H. Clinical aspects of argyrophilic grain disease. Clin Neuropathol 2000;19:278–84
19. Folstein MF, Folstein SE, McHugh PR. "Mini-mental state". A practical method for grading the cognitive state of patients for the clinician. J Psychiatr Res 1975;12:189–98
20. Hasegawa K, Inoue K, Moriya K. An investigation of dementia rating scale for the elderly. Seishin Igaku 1974;16:965–69
21. Katoh S, Simogaki H, Onodera A, et al. Development of the revised version of Hasegawa's dementia scale (HDS-R). Rounen Seishinigaku Zashi 1991;2:1339–47
22. Hughes CP, Berg L, Danziger WL, Coben LA, Martin RL. A new clinical scale for the staging of dementia. Br J Psychiatry 1982; 140:566–72
23. Mirra SS, Heyman A, McKeel D, et al. The Consortium to Establish a Registry for Alzheimer's Disease (CERAD). Part II. Standardization of the neuropathologic assessment of Alzheimer's disease. Neurology 1991;41:479–86
24. Braak H, Braak E, Ohm T, Bohl J. Silver impregnation of Alzheimer's neurofibrillary changes counterstained for basophilic material and lipofuscin pigment. Stain Technol 1988;63:197–200
25. Yamaguchi H, Haga C, Hirai S, Nakazato Y, Kosaka K. Distinctive, rapid, and easy labeling of diffuse plaques in the Alzheimer brains by a new methenamine silver stain. Acta Neuropathol 1990;79: 569–72
26. Saito Y, Kawai M, Inoue K, et al. Widespread expression of α-synuclein and τ immunoreactivity in Hallervorden-Spatz syndrome with protracted clinical course. J Neurol Sci 2000;177:48–59
27. Grogan TM, Casey TT, Miller PC, Rangel CS, Nunnery DW, Nagle RB. Automation of immunohistochemistry. Adv Pathol Lab Med 1993;6:253–83
28. Grogan TM, Rangel C, Rimsza L, et al. Kinetic-mode, automated double-labeled immunohistochemistry and in situ hybridization in diagnostic pathology. Adv Pathol Lab Med 1995;8:79–100
29. Wenham PR, Price WH, Blandell G. Apolipoprotein E genotyping by one-stage PCR. Lancet 1991;337:1158–59
30. Jellinger KA. Dementia with grains (argyrophilic grain disease). Brain Pathol 1998;8:377–86
31. The National Institute on Aging, and Reagan Institute Working Group on Diagnostic Criteria for the Neuropathological Assessment of Alzheimer's Disease. Consensus recommendations for the postmortem diagnosis of Alzheimer's disease. Neurobiol Aging 1997; 18:S1–S2
32. McKeith IG, Galasko D, Kosaka K, et al. Consensus guidelines for the clinical and pathologic diagnosis of dementia with Lewy bodies (DLB): Report of the consortium on DLB international workshop. Neurology 1996;47:1113–24
33. Chui HC, Victoroff JI, Margolin D, Jagust W, Shankle R, Katzman R. Criteria for the diagnosis of ischemic vascular dementia proposed by the State of California Alzheimer's Disease Diagnostic and Treatment Centers. Neurology 1992;42:473–80
34. Roman GC, Tatemichi TK, Erkinjuntti T, et al. Vascular dementia: Diagnostic criteria for research studies. Report of the NINDS-AIREN International Workshop. Neurology 1993;43:250–60
35. Amaral DG, Insausti R. Hippocampal formation. In: Paxinos G, ed. The human nervous system. San Diego: Academic Press, 1990: 711–55
36. Gloor P. The hippocampal system. In: Gloor P, ed. The temporal lobe and limbic system. Oxford: Oxford University Press, 1997: 325–589
37. Nieuwenhuys R, Voogd J, Huijzen C. The human central nervous system. 3rd ed. Berlin: Springer-Verlag, 1988
38. Braak H, Braak E. Argyrophilic grain disease: Frequency of occurrence in different age categories and neuropathological diagnostic criteria. J Neural Transm 1998;105:801–19
39. Dickson DW, Ksiezak-Reding H, Davies P, Yen SH. A monoclonal antibody that recognizes a phosphorylated epitope in Alzheimer neurofibrillary tangles, neurofilaments and tau proteins immunostains granulovacuolar degeneration. Acta Neuropathol (Berl) 1987; 73:254–58
40. Saito Y, Yamazaki M, Kanazawa I, Murayama S. Severe involvement of the ambient gyrus in a case of dementia with argyrophilic grain disease. J Neurol Sci 2002;196:71–75
41. Braak H, Del Tredici K, Bohl J, Bratzke H, Braak E. Pathological changes in the parahippocampal region in select non-Alzheimer's dementias. Ann N Y Acad Sci 2000;911:221–39
42. Braak H, Braak E. Neuropathological stageing of Alzheimer-related changes. Acta Neuropathol 1991;82:239–59

Received December 20, 2001
Revision received May 20, 2002
Accepted May 22, 2002